Speed Estimation of an Induction Motor Drive Using an Optimized Extended Kalman Filter

K. L. Shi, T. F. Chan, *Member, IEEE*, Y. K. Wong, *Senior Member, IEEE*, and S. L. Ho

***Abstract*—This paper presents a novel method to achieve good performance of an extended Kalman filter (EKF) for speed estimation of an induction motor drive. A real-coded genetic algorithm (GA) is used to optimize the noise covariance and weight matrices of the EKF, thereby ensuring filter stability and accuracy in speed estimation. Simulation studies on a constant V/Hz controller and a field-oriented controller (FOC) under various operating conditions demonstrate the efficacy of the proposed method. The experimental system consists of a prototype digital-signal-processor-based FOC induction motor drive with hardware facilities for acquiring the speed, voltage, and current signals to a PC. Experiments comprising offline GA training and verification phases are presented to validate the performance of the optimized EKF.**

***Index Terms*—Genetic algorithm, induction motor, Kalman filter.**

NOMENCLATURE

A_n, B_n, C_n	Input and output matrices of discrete system.
G	Weighting matrix of noise.
H	Matrix of output prediction.
i_{ds}, i_{qs}	Components of the stator current vector in the stator reference frame, A.
i_{Ds}, i_{Qs}	Components of the stator current vector in the excitation reference frame, A.
J_M	Moment of inertia of the rotor, kg·m^2.
J_L	Moment of inertia of the load, kg·m^2.
K_n	Kalman filter gain.
L_s	Stator inductance, H/phase.
L_M	Mutual inductance, H/phase.
L_r	Rotor inductance, H/phase.
M	Sampling period, s.
P	Number of poles.
P_n	Error covariance matrix.
Q	Covariance matrix of system noise.
R	Covariance matrix of measurement noise.
R_s	Stator resistance, Ω/phase.
R_r	Rotor resistance, Ω/phase.
T^*	Torque command, N·m.
T_L	Load torque, N·m.
u	Control function, vector.
$v(t)$	Noise matrix of output model.
V_{ds}, V_{qs}	Components of the stator voltage vector in the stator reference frame, V.
V_{Ds}, V_{Qs}	Components of the stator voltage vector in the excitation reference frame, V.
$w(t)$	Noise matrix of state model.
x	System state.
y	System output.
X_{ls}	Stator leakage reactance.
X_{lr}	Rotor leakage reactance referred to stator.
X_m	Magnetizing reactance.
ω_o, ω_o^*	Rotor speed and speed command, rad/s.
$\lambda_{dr}, \lambda_{qr}$	Components of the rotor flux vector, Wb.
$\lambda_{ds}, \lambda_{qs}$	Components of the stator flux vector, Wb.
Φ	Matrix of state prediction.

Manuscript received June 1, 2000; revised July 5, 2001. Abstract published on the Internet December 5, 2001. This work was supported by The Hong Kong Polytechnic University under Research Grant V157.

K. L. Shi was with the Department of Electrical Engineering, The Hong Kong Polytechnic University, Kowloon, Hong Kong. He is now with the Electrical and Computer Engineering Department, Ryerson Polytechnic University, Toronto, ON M5B 2K3 Canada (e-mail: shikeli@sympatico.ca).

T. F. Chan, Y. K. Wong, and S. L. Ho are with the Department of Electrical Engineering, The Hong Kong Polytechnic University, Kowloon, Hong Kong (email: eetfchan@polyu.edu.hk; eeykwong@polyu.edu.hk; eeslho@polyu.edu.hk).

Publisher Item Identifier S 0278-0046(02)00929-2.

I. INTRODUCTION

SPEED estimation methods have in recent years aroused great interest among induction motor control researchers. From the drive system's point of view, elimination of the speed sensors and the associated measurement cables has the advantages of lower cost, ruggedness, as well as increased reliability. Compared with a nonlinear observer [1], the Kalman filter has a good dynamic behavior, disturbance resistance, and it can work even under standstill conditions. The Kalman filter is a special kind of observer that provides optimal filtering of the noises in measurement and inside the system if the covariances of these noises are known. The extended Kalman filter (EKF) is based on the nonlinear extended induction motor model that includes the rotor speed as a state variable. Although considerable progress has been achieved for EKF induction motor drives [2]–[4], little attempt has been made to optimize the filter performance. As the correct noise matrices cannot be chosen based on classical theories, they are usually tuned experimentally by a trial-and-error method [1], [5]—a tedious process which may not give accurate results. In this paper, a real-coded genetic algorithm (GA) [6], [7] is employed for optimizing the noise covariance matrices in order to achieve the best EKF performance. Simulation studies are carried out on a closed-loop constant V/Hz controller and a field-oriented controller (FOC) to justify the need for an optimized EKF. An induction motor drive with FOC, implemented based on a fixed-point digital signal processor (DSP), is used for the experimental investigations. Simulation and experimental results will be presented to confirm the efficacy of the GA-optimized EKF for speed estimation in induction motor drives.

II. Extended State Model of Induction Motor

A dynamic electrical model for a three-phase induction motor has four state variables, namely, the stator currents (i_{ds}, i_{qs}) and the rotor fluxes ($\lambda_{dr}, \lambda_{qr}$). An extended induction motor model results if the rotor speed is included as an additional state variable. The extended model can be expressed as follows [8]:

$$\dot{x} = Ax + Bu + G(t)w(t) \quad \text{(system)} \tag{1}$$

$$y = Cx + v(t) \quad \text{(Measurement)} \tag{2}$$

where

$$x_n = \begin{bmatrix} i_{ds}^{(n)} \\ i_{qs}^{(n)} \\ \lambda_{dr}^{(n)} \\ \lambda_{qr}^{(n)} \\ \omega_o^{(n)} \end{bmatrix}$$

$$y_n = \begin{bmatrix} i_{ds}^{(n)} \\ i_{qs}^{(n)} \end{bmatrix}$$

$$u = \begin{bmatrix} V_{ds}^{(n)} \\ V_{qs}^{(n)} \end{bmatrix}$$

$$A_n = \begin{bmatrix} 1-\frac{K_r}{K_l}M & 0 & \frac{L_M R_r}{L_r^2 K_l}M & \frac{PL_M\omega_o^{(n)}}{2L_r K_l}M & 0 \\ 0 & 1-\frac{K_r}{K_l}M & \frac{PL_M\omega_o^{(n)}}{2L_r K_l}M & \frac{L_M R_r}{L_r^2 K_l}M & 0 \\ \frac{L_M}{\tau_r}M & 0 & 1-\frac{1}{\tau_r}M & -\frac{P}{2}\omega_o^{(n)}M & 0 \\ 0 & \frac{L_M}{\tau_r}M & \frac{P}{2}\omega_o^{(n)}M & 1-\frac{1}{\tau_r}M & 0 \\ 0 & 0 & 0 & 0 & 1 \end{bmatrix}$$

$$B_n = \begin{bmatrix} \frac{M}{K_l} & 0 \\ 0 & \frac{M}{K_l} \\ 0 & 0 \\ 0 & 0 \\ 0 & 0 \end{bmatrix}$$

$$C_n = \begin{bmatrix} 1 & 0 & 0 & 0 & 0 \\ 0 & 1 & 0 & 0 & 0 \end{bmatrix}.$$

In matrices A_n and B_n, $\tau_r = L_r/R_r$, $K_r = R_s + L_M^2 R_r/L_r^2$ and $K_l = (1 - L_M^2/L_r/L_s)^* L_s$.

In (1) and (2), $G(t)$ is the noise–weight matrix, $w(t)$ is the noise matrix of state model (system noise), and $v(t)$ is the noise matrix of output model (measurement noise). The covariance matrices Q and R of these noises are defined as

$$Q = \text{cov}(w) = E\{ww^t\} \tag{3}$$

$$R = \text{cov}(v) = E\{vv^t\} \tag{4}$$

where $E\{.\}$ denotes the expected value.

III. EKF Algorithm for Rotor Speed Estimation

The recursive form of the Kalman filter may be expressed by the following system of equations, where all symbols in the formulations denote matrices or vectors [3].

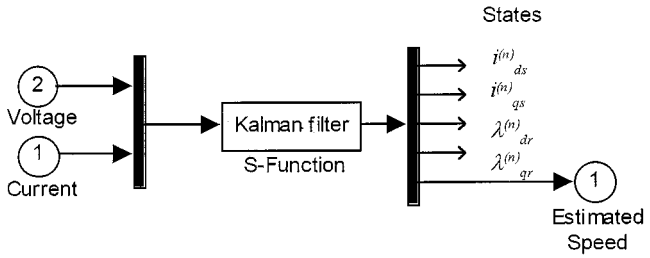

Fig. 1. Simulink model of extended Kalman filter speed estimator.

A. Prediction of State

$$x_{n+1\,n} = \Phi(n+1, n, x_{n\,n-1}, u_n) \tag{5}$$

where

$$\Phi(n+1, n, x_{nn-1}, u_n) = A_n(x_{nn})\,x_{nn} + B_n(x_{nn})\,u_n. \tag{6}$$

B. Estimation of Error Covariance Matrix

$$P_{n+1\,n} = \left.\frac{\partial \Phi}{\partial x}\right|_{x=x_{nn}} P_{nn} \left.\frac{\partial \Phi^T}{\partial x}\right|_{x=x_{nn}} + \Gamma_n Q \Gamma_n^T \tag{7}$$

where

$$\Gamma = \int_n^{n+1} \Phi(t_{n+1}, \tau)\, G(\tau) d\tau$$

and the initial value of P_{nn} is a constant matrix.

C. Computation of Kalman Filter Gain

$$K_n = P_{nn-1} \left.\frac{\partial H^T}{\partial x}\right|_{x=x_{nn-1}} \cdot \left(\left.\frac{\partial H}{\partial x}\right|_{x=x_{nn-1}} P_{nn-1} \left.\frac{\partial H^T}{\partial x}\right|_{x=x_{nn-1}} + R \right)^{-1} \tag{8}$$

where

$$H(x_{nn-1}, n) = C_n(x_{nn-1})\,x_{nn-1}. \tag{9}$$

D. State Estimation

$$x_{nn} = x_{nn-1} + K_n\left(y_n - H\left(x_{nn-1}, n\right)\right). \tag{10}$$

E. Update of the Error Covariance Matrix

$$P_{nn} = P_{nn-1} - K_n \left.\frac{\partial H}{\partial x}\right|_{x=x_{nn-1}} P_{nn-1}. \tag{11}$$

In this paper, simulation studies on the speed estimation algorithm of the EKF are performed on a PC using the Matlab/Simulink software, as illustrated in Fig. 1. For convenience, the EKF algorithm is coded in an M-file (written in the Matlab language) which is placed in the S-function block [9]. The EKF algorithm is executed whenever the S-function is called.

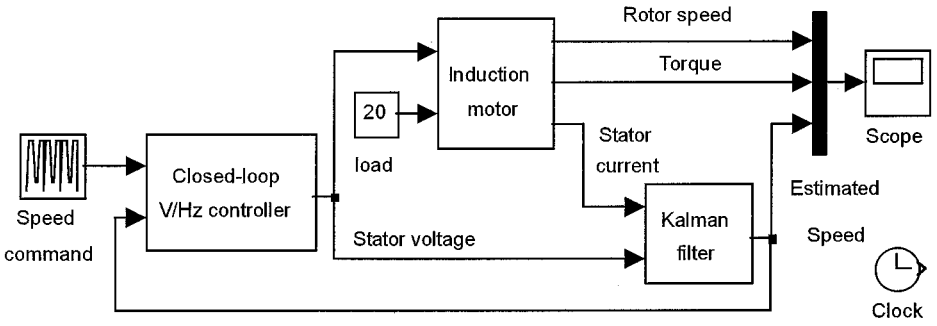

Fig. 2. Closed-loop constant V/Hz control system with EKF speed estimation.

IV. Optimization of EKF

To justify the need for an optimized EKF, the EKF speed estimation algorithm is applied to a closed-loop constant V/Hz controller [10] as shown in Fig. 2.

The induction motor used for the simulation studies has the following parameters. Type: three-phase six-pole 60-Hz 7.5-kW 220-V squirrel-cage induction motor

$$R_S = 0.288\ \Omega/\text{phase}\ R_r = 0.161\ \Omega/\text{phase}$$
$$X_{ls} = 0.512\ \Omega/\text{phase}\ X_{lr} = 0.218\ \Omega/\text{phase}$$
$$X_M = 14.821\ \Omega/\text{phase}\ J_M = 0.4\ \text{kg}\cdot\text{m}^2$$
$$J_L = 0.4\ \text{kg}\cdot\text{m}^2\ T_L = 20\ \text{N}\cdot\text{m}.$$

In the simulation, the error covariance matrix P of the EKF is initially set as a unit matrix while the noise covariance matrices R, Q, and noise–weight matrix G are assumed as

$$P = \begin{bmatrix} 1 & 0 & 0 & 0 & 0 \\ 0 & 1 & 0 & 0 & 0 \\ 0 & 0 & 1 & 0 & 0 \\ 0 & 0 & 0 & 1 & 0 \\ 0 & 0 & 0 & 0 & 1 \end{bmatrix}$$
$$R = \begin{bmatrix} 10^{-3} & 0 \\ 0 & 10^{-3} \end{bmatrix}$$
$$Q = \begin{bmatrix} \xi & 0 & 0 & 0 & 0 \\ 0 & \xi & 0 & 0 & 0 \\ 0 & 0 & \xi & 0 & 0 \\ 0 & 0 & 0 & \xi & 0 \\ 0 & 0 & 0 & 0 & \delta \end{bmatrix}$$
$$G = \begin{bmatrix} \lambda & 0 & 0 & 0 & 0 \\ 0 & \lambda & 0 & 0 & 0 \\ 0 & 0 & \lambda & 0 & 0 \\ 0 & 0 & 0 & \lambda & 0 \\ 0 & 0 & 0 & 0 & \mu \end{bmatrix}.$$

The values of ξ, δ, λ and μ in matrices Q and G are usually determined using a trial-and-error process. For comparison purposes, the performance of the EKF with different compositions of Q and G is evaluated by the mean-squared error between the estimated speed and the actual rotor speed. Since the estimated speed ω_o in (1) generally experiences greater variations than the other state variables, it is logical to assign greater values to μ and δ (which correspond to the noise of the estimated speed) in the covariance matrices G and Q,. Table I shows typical EKF performance obtained by a trial-and-error method. It is found that poor speed estimation performance results when the parameters λ, μ, ξ and δ are equal (Cases 1–3). By selecting larger values of δ and μ relative to ξ and λ, the EKF performance is improved (Cases 4 and 5). Good speed estimation performance is obtained with the matrix $Q = Diag[10^{-6}, 10^{-6}, 10^{-6}, 10^{-6}, 10^{-2}]$ and $G = Diag[10^{-6}, 10^{-6}, 10^{-6}, 10^{-6}, 10^{-2}]$ (Case 6). Fig. 3 shows the estimated speed of the EKF for Cases 1, 2, 3, and 6. The results are consistent with the observation made with reference to Table I.

TABLE I
Performance of EKF for a Constant V/Hz Induction Motor Drive

Case	Matrices G and Q	$E = \frac{1}{n}\sum_{i=1}^{n}(s_i - e_i)^2$	Estimation results
1	$\lambda=\mu=\xi=\delta=1e\text{-}2$	417.1220	Poor
2	$\lambda=\mu=\xi=\delta=1e\text{-}3$	772.4852	Poor
3	$\lambda=\mu=\xi=\delta=1e\text{-}6$	2.5927e+003	Poor
4	$\lambda=\xi=\delta=1e\text{-}3$, $\mu=1e\text{-}2$	1.5331	Good
5	$\lambda=\xi=1e\text{-}3$, $\mu=\delta=1e\text{-}2$	1.0164	Good
6	$\lambda=\xi=1e\text{-}6$, $\mu=\delta=1e\text{-}2$	0.9985	Very good

s = actual rotor speed, e = estimated speed,
n = number of data samples (= 45000),
E = mean squared error of estimated speed.

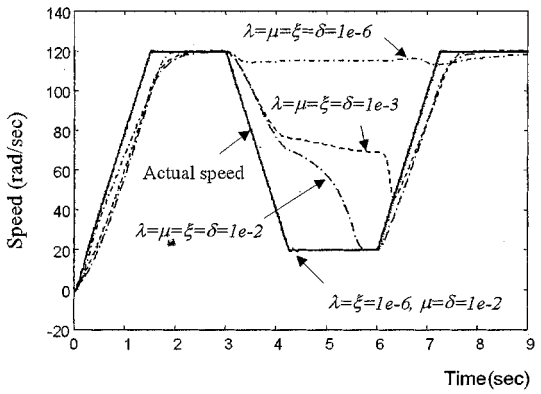

Fig. 3. Performance of EKF for the constant V/Hz induction motor drive with various covariance matrices (solid line: actual speed; dotted line: estimated speed).

Manual tuning of the EKF using the trial-and-error method is simple to carry out, but the process is very time consuming and satisfactory performance can only be obtained with great effort from an experienced operator. As the distribution of noise is usually unknown, it is not possible to deduce a generic relationship

between the values of the matrix elements and the EKF performance for fine tuning of the matrices to yield the best speed estimation results.

V. Optimizing the Noise Matrices of EKF Using a GA

When the speed estimation technique is implemented in a practical closed-loop sensorless induction motor drive, the significant delay between actual speed and EKF estimation speed will result in large speed oscillations. The difficulties in applying the EKF speed estimation technique may be overcome by the use of a GA which has evolved as a powerful optimization tool over the past three decades [11]. A GA is a stochastic global search method that mimics the metaphor of natural biological evolution. The algorithm differs substantially from more traditional search and optimization methods as follows.

1) A GA searches a population of points in parallel instead of searching for a single point.
2) A GA does not require derivative information or other auxiliary knowledge; only the objective function and corresponding fitness levels influence the directions of search.
3) A GA uses probabilistic transition rules instead of deterministic rules.
4) The nature of the function being optimized is immaterial: both unimodal and multimodal functions can be dealt with successfully. The parallel search capability of a GA avoids the iterations being trapped in local optimum points.

Among the four matrices in the EKF speed estimation algorithm, the error covariance matrix P will be updated in the course of the EKF iterations as prescribed by (10), which implies that only matrices G, Q, and R need to be optimized. For this purpose, an optimization method based on a real-coded GA [7] is employed in this paper. Compared with a binary-coded GA, a real-coded GA is more efficient as there is no need to convert chromosomes to phenotypes before each fitness evaluation. Less memory is required and there is no loss in precision caused by the conversion between binary and real values. The procedures of the real-coded GA are outlined as follows.

1) Population Representation of the Natural Parameter: The five diagonal elements (G_d) of the matrix G, five diagonal elements (Q_d) of covariance matrix Q, and two diagonal elements (R_d) of covariance matrix R are coded into a long real-valued string, known as a *chromosome*. A typical coding example of a chromosome is given as follows:

$$\begin{aligned} G_d &= [0.0637, 0.0769, 0.0054, 0.0115, 0.0846] \\ Q_d &= [0.0172, 0.0037, 0.0313, 0.0817, 0.0235] \\ R_d &= [0.0587, 0.0924] \\ chromosome &= [G_d, Q_d, R_d] \\ &= [0.0637, 0.0769, 0.0054, 0.0115, 0.0846, 0.0172, \\ &\quad 0.0037, 0.0817, 0.0235, 0.0587, 0.0924]. \end{aligned}$$

2) Initial Generation: The GA begins by randomly generating an initial population of the long real-valued strings.

3) Fitness Evaluation: In the current generation, each of the strings is decoded back to the corresponding diagonal elements of the three matrices, G_d, Q_d and R_d. Then, these diagonal elements from each string are separately sent to the EKF speed estimator of the induction motor drive to yield the objective function (which is the mean squared error of the estimated speed). Finally, these strings are ranked according to the value of the objective function by a linear ranking method.

4) Reproduction: Reproduction is a process by which parent structures are selected to form new offspring. In this paper, the stochastic universal sampling method is employed.

5) Recombination (Crossover): The single-point recombination method is used to exchange the information between two chromosomes.

6) Mutation: The Breeder Genetic Algorithm [12] is used to implement the mutation operator for the real-coded GA, which uses a nonlinear term for the distribution of the range of mutation applied to gene values. This mutation algorithm is able to generate most points in the hypercube defined by the variables of the individual and range of the mutation. By biasing mutation toward smaller changes in gene values, the mutation can be used in conjunction with recombination as a foreground search process.

7) Iteration: The real-coded GA runs iteratively repeating the procedures 3)–7) until a population convergence condition is met or the maximum number of iterations is reached.

The real-coded GA for the EKF (GA-EKF) has been implemented using Matlab/Simulink. For optimizing the covariance matrices G, Q, and R of the EKF, the parameters of the GA are set as follows:

1) initial population size—100;
2) maximum number of generations—20;
3) probability of crossover—0.8;
4) putation probability—0.01;
5) initial range of real-valued strings—[0.0001; 0.1];
6) performance measure—the mean-squared error between the estimated speed and the actual rotor speed.

The training set for the GA optimization process consists of the stator voltages (V_{ds}, V_{qs}) and the stator currents (i_{ds}, i_{qs}) of the closed-loop constant V/Hz drive. This training set is input to the EKF speed estimator, while the actual rotor speed of the motor drive is taken to be the target set for *Fitness evaluation* by the GA. In order to cover both the transient and steady-state operations of the induction motor drive, the training sequence of 45 000 vectors [$V_{ds}, V_{qs}, i_{ds}, i_{qs}, \omega_o$] is sampled over the following speed command periods:

$$\begin{aligned} \omega_o^* &= 0 \sim 120 \text{ rad/s}, & 0 \text{ s} < t \le 1.5 \text{ s} \\ \omega_o^* &= 120 \text{ rad/s}, & 1.5 \text{ s} < t \le 3 \text{ s} \\ \omega_o^* &= 120 \sim 20 \text{ rad/s}, & 3 \text{ s} < t \le 4.25 \text{ s} \\ \omega_o^* &= 20 \text{ rad/s}, & 4.25 \text{ s} < t \le 5 \text{ s}. \end{aligned}$$

The training sequence thus includes sufficient information on the dynamics of the practical drive for the GA to optimize the EKF noise matrices for operation with various speed commands.

TABLE II
OPTIMIZING EKF PERFORMANCE USING GA FOR THE CONSTANT V/HZ INDUCTION MOTOR DRIVE

Generations	$E=\frac{1}{n}\sum_{i=1}^{n}(s_i-e_i)^2$	Generations	$E=\frac{1}{n}\sum_{i=1}^{n}(s_i-e_i)^2$
0	8.3137		
1	5.2311	11	0.5713
2	3.8212	12	0.5247
3	2.9570	13	0.3943
4	2.3951	14	0.3306
5	1.5648	15	0.2425
6	0.9142	16	0.1794
7	0.8853	17	0.1731
8	0.7271	18	0.1618
9	0.6370	19	0.1662
10	0.6286	20	0.1543

s = actual rotor speed, e = estimated speed,
n = number of data samples (= 45000),
E = best mean squared error of estimated speed in each generation.

When the size of the initial population is small, the GA may not always converge or arrive at the optimal solution within a limited number of iterations [12]. For the 12-dimensional search space formed by the diagonal elements of the matrices G, Q, and R, an initial population size of 100 or more has to be chosen in order to give satisfactory results. It should be noted, however, that the GA-EKF algorithm is computationally intensive. The computation time for one generation (with a population size of 100) is about 8 h on a PII 350 PC. In view of the computing facilities available, the maximum number of generations is limited to 20 and the off-diagonal elements of the matrices have not been investigated.

Table II shows the convergence process of the real-coded GA, where E denotes the best (minimum) mean-squared error in each generation. After 20 generations, E is reduced to 0.1543 with the optimized matrices $G = Diag[0.0020\ 0.0050\ 0.0010\ 0.0246\ 0.1000]$, $Q = Diag[0.0024\ 0.0875\ 0.0527\ 0.0001\ 0.0978]$, and $R = Diag[0.0524\ 0.0094]$. A marked improvement in the EKF performance is, thus, achieved with the GA optimization approach.

A closer examination of Table II reveals that the values of E may not decrease monotonically with the number of generations. This is caused by the *Mutation* operation [13] whose function is to guarantee that the probability of searching any given string will never be zero. It therefore acts as a safety net to recover good genetic material that may be lost through the action of *Reproduction* and *Recombination* (*Crossover*).

Figs. 4 and 5 show the EKF performance for the closed-loop constant V/Hz controller with the matrices tuned by the trial-and-error method (when $\lambda = \xi = 1e-6$ and $\delta = \mu = 1e-2$) and matrices optimized by the GA, respectively. For comparison purposes, the same control cycle is used for both cases. The simulation results show that the EKF optimized by the GA gives more accurate speed estimation compared with an EKF tuned by the trial-and-error method.

Since the EKF matrices have been optimized with respect to the given induction motor, the performance of the EKF is satisfactory for various modes of drive operation. Fig. 6 shows

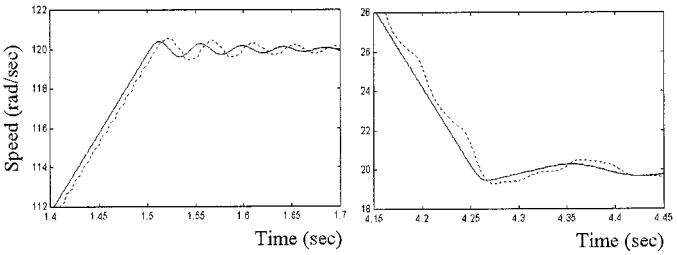

Fig. 4. Actual speed and estimated speed of the constant V/Hz controller: EKF matrices tuned by trial-and-error method ($\lambda = \xi = 1e-6$ and $\delta = \mu = 1e-2$) (solid line: actual speed; dotted line: estimated speed).

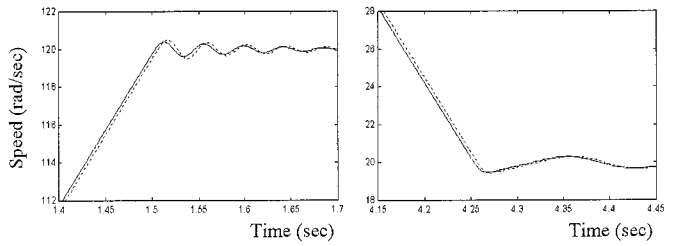

Fig. 5. Actual speed and estimated speed of the constant V/Hz controller: EKF matrices optimized by GA (solid line: actual speed; dotted line: estimated speed).

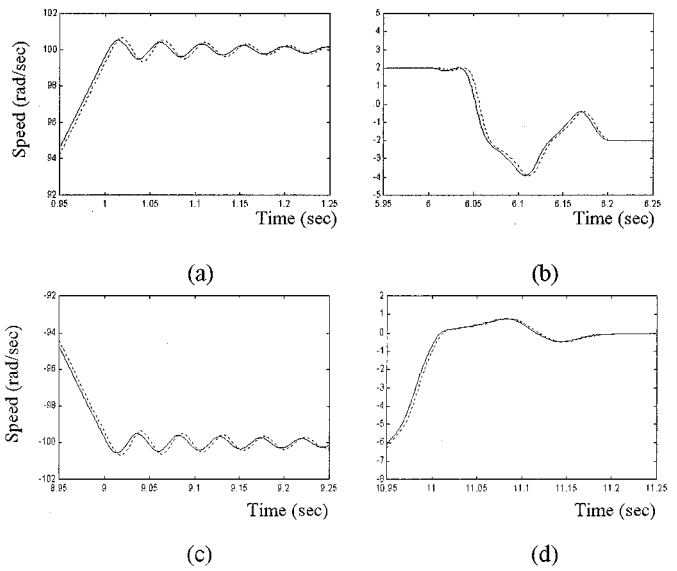

Fig. 6. Performance of GA-optimized EKF of the constant V/Hz drive with various speed control commands (solid line: actual speed; dotted line: estimated speed). (a) Acceleration to 100 rad/s. (b) Speed reversal from 2 to -2 rad/s. (c) Acceleration to -100 rad/s. (d) Deceleration to standstill.

the simulation results of the optimized EKF for the constant V/Hz controller for different speed commands. It is observed that accurate speed tracking is possible at different speeds and even under standstill conditions.

It is of interest to investigate the effect of machine parameter changes (e.g., due to temperature rise) on the EKF performance. For this purpose, the motor resistances used in the EKF model are kept constant at their nominal values R_s and R_r. Fig. 7 shows the rotor speed response of the constant V/Hz controller and the estimated speed of the optimized EKF when the motor resistances are increased. The extended Kalman filter shows disturbance rejection to the machine parameter variations because

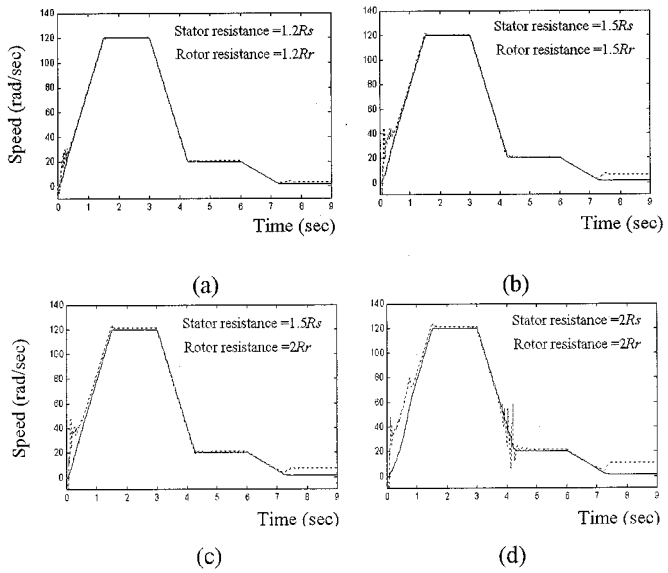

Fig. 7. Performance of GA-optimized EKF of the constant V/Hz controller with machine parameter variations (solid line: actual speed; dotted line: estimated speed).

the latter are handled as noise in the speed estimation algorithm. The accuracy of speed tracking is good even when the stator resistance is increased by 50% and the rotor resistance is doubled [Fig. 7(c)].

VI. Speed Estimation for an FOC

To further evaluate the performance of the optimized EKF, speed estimation for an FOC induction motor drive is also investigated. Fig. 8 shows the block diagram of the FOC system with direct stator flux orientation [14]. From the stator voltages (V_{ds}, V_{qs}) and stator currents (i_{ds}, i_{qs}), the stator flux can be obtained by a "Flux calculate" block based on the following equations for a voltage-input induction motor model [15]:

$$\lambda_{ds} = \int (V_{ds} - R_s i_{ds})\, dt \tag{12}$$

$$\lambda_{qs} = \int (V_{qs} - R_s i_{qs})\, dt \tag{13}$$

$$|Flux| = \sqrt{\lambda_{ds}^2 + \lambda_{qs}^2} \tag{14}$$

$$\alpha = \tan^{-1}\left(\frac{\lambda_{ds}}{\lambda_{qs}}\right). \tag{15}$$

Two proportional–integral (PI) blocks control the stator flux and rotor speed, while another two PI blocks control the stator currents (i_{Ds}, i_{Qs}) in field coordinates. Coordinate transformation of voltages from the field frame (V_{Ds}, V_{Qs}) to the stator frame (V_{ds}, V_{qs}) is implemented by an inverse Park calculation. At the same time, the three-phase voltage signals and three-phase current signals are sent to the GA-EKF block for rotor speed estimation.

Simulation studies are performed on the experimental FOC drive system. The three-phase four-pole squirrel-cage induction motor is rated at 220 V, 150 W, 60 Hz and has the following parameters:

$$\begin{aligned} R_S &= 14.6\,\Omega/\text{phase}\ R_r = 12.77\,\Omega/\text{phase} \\ X_{ls} &= 8.37\,\Omega/\text{phase}\ X_{lr} = 19.53\,\Omega/\text{phase} \\ X_M &= 111.7\,\Omega/\text{phase}\ J_M = 0.0028\,\text{kg}\cdot\text{m}^2 \\ J_L &= 0.01\,\text{kg}\cdot\text{m}^2\ T_L = 0.5\,\text{N}\cdot\text{m}. \end{aligned}$$

The training sequence and parameters of the GA for optimizing the EKF matrices G, Q, and R are the same as those in Section V except that the initial range of the real-valued strings is set as [0.01; 5]. A different initial range is necessary in order to guarantee convergence and short iteration time.

Table III shows the convergence process of the real-coded GA for the FOC drive. At the 20th generation, the minimum mean-squared error of the estimated speed has decreased to 0.1489 with the optimized matrices $G = Diag[0.0143\ 0.0754\ 0.0326\ 0.1635\ 3.2662]$, $Q = Diag[0.0132\ 0.0538\ 0.0724\ 0.0081\ 1.4672]$ and $R = Diag[0.0163\ 0.0085]$. Fig. 9(a) shows the performance of the GA-optimized EKF for the FOC induction motor drive subjected to a typical load cycle, while Fig. 9(b)-(f) shows the various modes of drive operation in different time intervals, suitable speed scales having been used to highlight the speed-tracking capability of the EKF. The GA-optimized EKF gives excellent performance over the entire speed range, including constant-speed operation [Fig. 9(b)], low-speed operation [Fig. 9(d)], and even with the drive at standstill [Fig. 9(f)]. Accuracy of speed estimation is also good under rapid acceleration and deceleration transients [Fig. 9(c) and 9(e)].

The optimized EKF also gives satisfactory performance when the load changes. Fig. 10(a) shows the speed estimation performance following a change in load torque from 0.5 to 1.0 N·m with the motor drive operating at high speed. There is a short period during which the estimated speed fails to track the actual speed due to voltage and current transients. A similar transient period occurs when the load torque is reduced from 1.0 to 0.5 N·m with the motor operating at a very low speed, but the percentage error is now considerably larger. In both cases, however, the EKF starts to give accurate estimation of speed again 0.04 s after the change in load torque.

VII. Experimental System

Experimental investigation on the EKF involves acquisition of stator voltages, stator currents and rotor speed of the FOC induction motor drive to a PC for offline optimization of the matrices G, Q, and R of the EKF using GA. The optimized EKF is then used for speed estimation of the drive. A comparison of the estimated speed with the actual speed of the induction motor enables the efficacy of the GA-optimized EKF to be ascertained.

Fig. 11 shows the experimental DSP-based FOC drive system with data acquisition for optimization of the EKF. The system consists of an ADMC331 fixed-point DSP board (Analog Devices Inc.), an insulated gate bipolar transistor

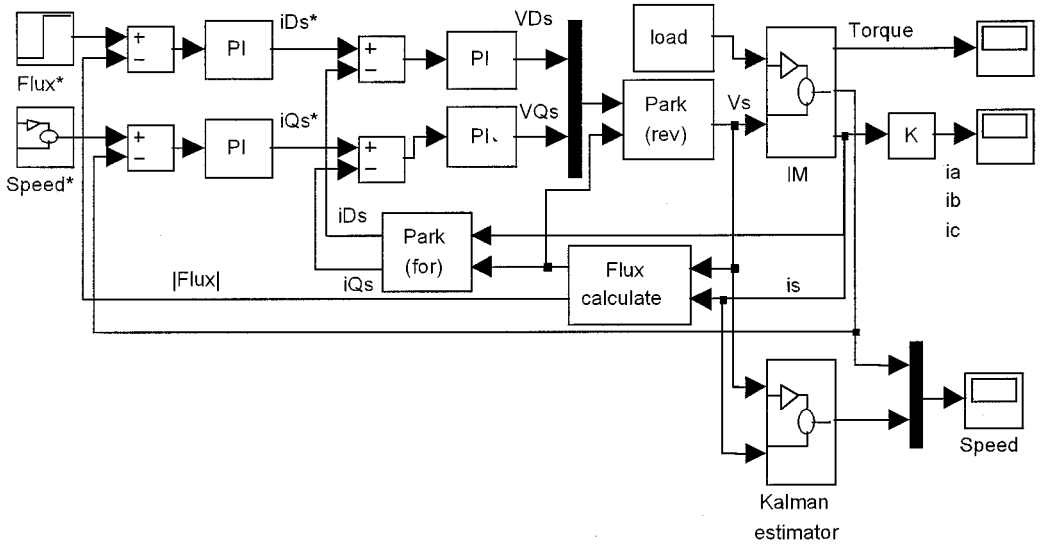

Fig. 8. Simulation of an FOC induction motor drive with EKF speed estimation.

TABLE III
OPTIMIZING EKF PERFORMANCE USING GA FOR THE FOC INDUCTION MOTOR DRIVE (SPEED DATA FROM SIMULATION USED AS TARGET FUNCTION)

Generations	$E=\frac{1}{n}\sum_{i=1}^{n}(s_i-e_i)^2$	Generations	$E=\frac{1}{n}\sum_{i=1}^{n}(s_i-e_i)^2$
0	15.960		
1	9.2410	11	0.6375
2	6.4387	12	0.5584
3	4.7395	13	0.4742
4	3.1094	14	0.4341
5	2.3400	15	0.3526
6	1.5067	16	0.2775
7	1.2093	17	0.2366
8	1.3210	18	0.1773
9	0.9344	19	0.1520
10	0.8471	20	0.1489

s = actual rotor speed, e = estimated speed,
n = number of data samples (= 45000),
E = best mean squared error of estimated speed in each generation.

(IGBT) inverter power module IRPT1058A (International Rectifier Inc.), a data acquisition board PCL818HG (Advantech Company Ltd.), an encoder GBZ02 with a resolution of 200 pulses/revolution (China Sichuan Opto-electronic Company), three-phase current sensor 3I411A (China WB institute), a PC , and a 150-W three-phase induction motor.

Besides the DSP unit ADSP-2171, the ADMC331 processor board also includes a motor control peripheral with 16-b three-phase pulsewidth modulation (PWM) generation unit. The DSP has a processor speed of 26 MIPS and provides 2K $\times$ 24-b program RAM, 2K $\times$ 24-b program ROM, and 1K $\times$ 16-b data RAM. The FOC program and data memories can be boot-loaded through an RS232 serial port. On a connector board of the ADMC331, a 12-b digital-to-analog converter (DAC) AD7568 delivers the stator voltage signals for EKF speed estimation. The three-phase current signals are obtained from the motor input leads via the 3I411A current sensors.

A PC-based data acquisition board PCL-818HG is used to acquire the required signals to a PC for the GA-EKF studies. It is a 12-b A/D converter with eight differential analog inputs

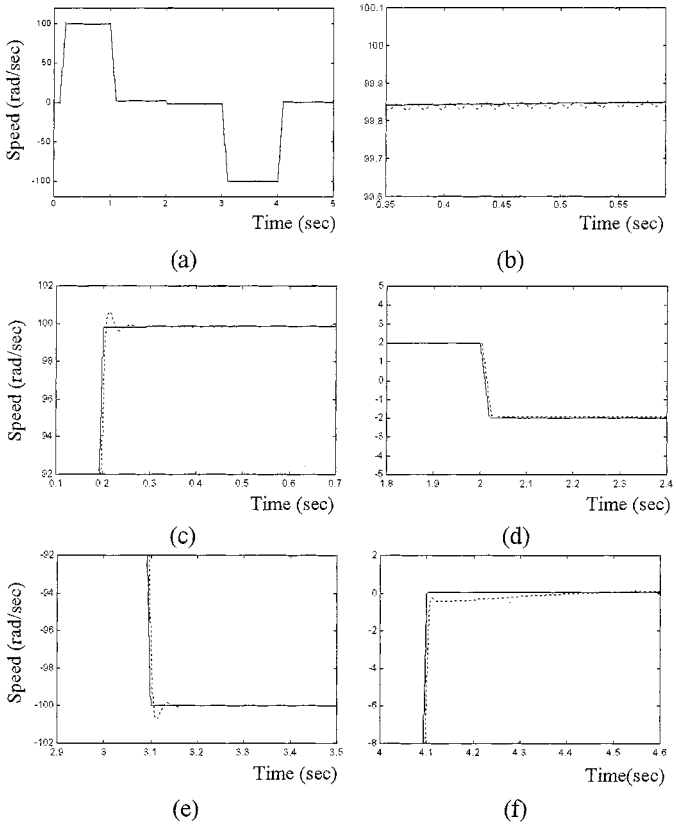

Fig. 9. Performance of the GA-optimized EKF for FOC drive (solid line: actual speed; dotted line: estimated speed). (a) Performance over a complete load cycle. (b) Constant-speed operation. (c) Acceleration to 100 rad/s. (d) Speed reversal from 2 to -2 rad/s. (e) Acceleration to -100 rad/s. (f) Deceleration to standstill.

and a conversion time of 25 μs. In the experimental studies, the phase voltages, phase currents, and rotor speed are input to the PC via seven channels at a sampling rate of 20 kHz using a direct memory access (DMA) program. The DMA method is capable of rapid data exchange by allowing external devices to transfer data directly to the PC memory without involving the interrupt commands of the system CPU.

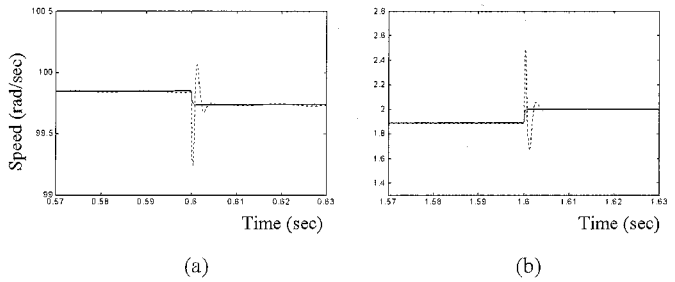

Fig. 10. Performance of the GA-optimized EKF for FOC drive with load change (solid line: actual speed; dotted line: estimated speed). (a) Load torque increased from 0.5 to 1 N·m, motor operating at high speed. (b) Load torque decreased from 1 to 0.5 N·m, motor operating at low speed.

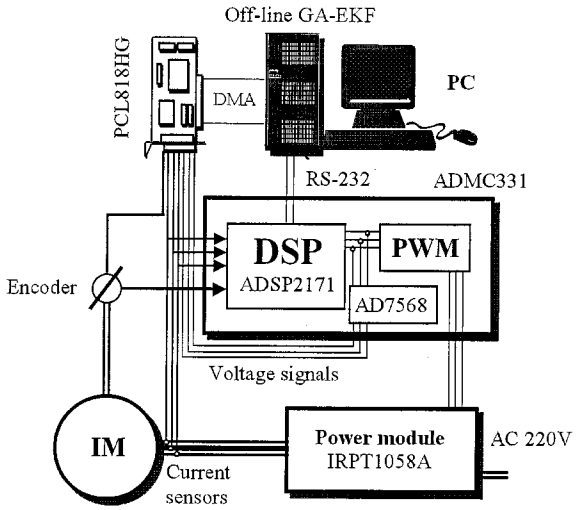

Fig. 11. Experimental FOC induction motor drive system with data acquisition for optimization of EKF.

The experimental FOC algorithm is the same as the simulation program with direct stator flux orientation as described in Section VI.

The GA-EKF experiment consists of the training phase and the verification phase. In the training phase, three-phase voltage and current are acquired as training samples from the experimental system and the actual rotor speed is acquired from the encoder as the target function. After the optimized matrices G, Q, and R have been obtained offline using the real-coded GA, the performance of the EKF is examined in the verification phase by comparison with the new acquired data samples.

Fig. 12 shows a block diagram of the GA procedure for the training phase while Fig. 13 shows the acquired phase voltage and phase current when the FOC drive is run up from standstill to 105 rad/s.

In order to account for the noise present in the actual drive system, the EKF need to be optimized again for the experimental studies. The parameters of the GA for optimizing the matrices G, Q, and R of EKF from the experimental data are the same as those in Section VI. Table IV shows the convergence process. The GA optimization method has improved the EKF performance by decreasing the mean squared error of estimated speed from 12.6931 to 1.2980. The mean-squared error is larger than that obtained in the previous simulation results, one

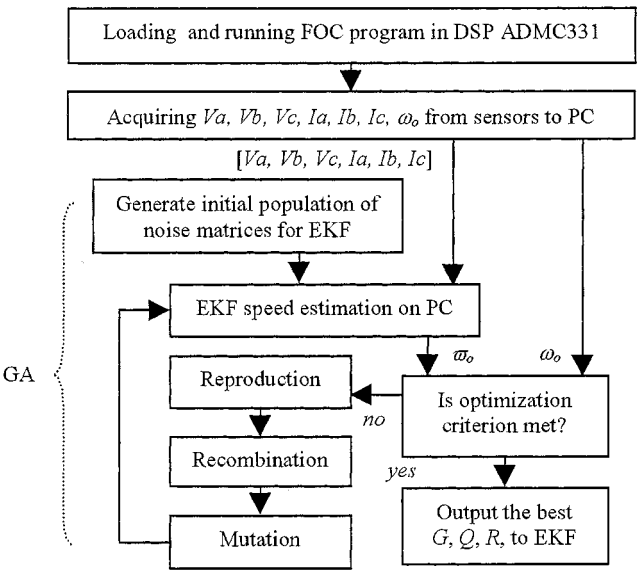

Fig. 12. Program flowchart for optimizing the EKF using GA in training phase.

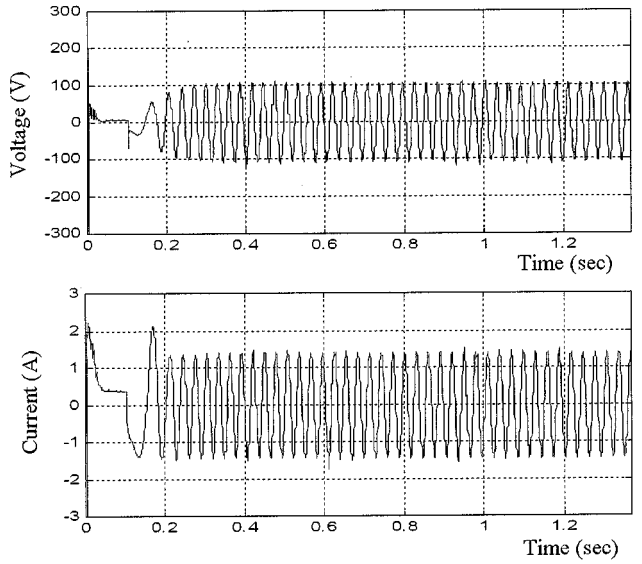

Fig. 13. Experimental phase voltage and phase current waveforms of the FOC drive when run up to 105 rad/s.

reason being that the experimental system can only deliver a training set of 4571 vector samples over a period of 1.4 s. In the simulation, however, the training set comprises 45 000 vector samples taken over a period of 5 s. The second reason is that practical noises of voltage and current are carried into the EKF from the experimental system and encoder noise is carried into the GA operator, whereas no account has been taken of system noise in the simulation program. The optimized matrices are $G = Diag[0.1264,\ 0.1306,\ 0.1847,\ 0.1945,\ 1.5603]$, $Q = Diag[0.0648,\ 0.0993,\ 0.0816,\ 0.0963,\ 1.5000]$ and $R = Diag[0.0101,\ 0.0104]$. Fig. 14 shows the actual speed and the speed estimated using the EKF with the optimized matrices. The initial switching transients in the voltage and current waveforms cause the estimated speed of the EKF to deviate from the actual rotor speed, but the discrepancy decreases with

TABLE IV
OPTIMIZING EKF PERFORMANCE USING GA FOR THE FOC DRIVE (SPEED DATA FROM EXPERIMENT USED AS TARGET FUNCTION)

Generations	$E = \frac{1}{n}\sum_{i=1}^{n}(s_i - e_i)^2$	Generations	$E = \frac{1}{n}\sum_{i=1}^{n}(s_i - e_i)^2$
0	12.6931		
1	4.0216	11	1.6493
2	4.3045	12	1.6320
3	3.1341	13	1.5234
4	3.0235	14	1.6019
5	2.8401	15	1.4820
6	2.5294	16	1.4397
7	2.1983	17	1.3589
8	2.2631	18	1.3740
9	1.9578	19	1.3138
10	1.8653	20	1.2980

s = actual rotor speed, e = estimated speed,
n = number of data samples (= 4571)
E = best mean squared error of estimated speed in each generation.

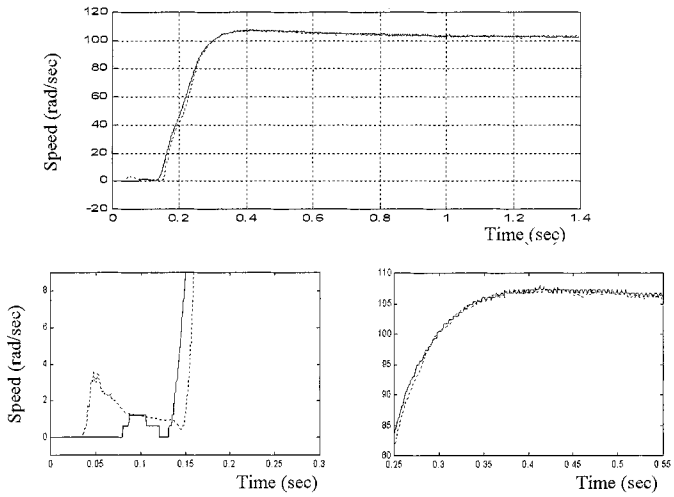

Fig. 14. Actual speed and speed estimated using the GA-optimized EKF when the FOC drive is run up to 105 rad/s (solid line: actual speed; dotted line: estimated speed).

time as the voltage and current settle to the values as specified by the controller.

In the verification phase, the FOC drive is run up from standstill to 188 rad/s. Data samples are acquired to the PC and the GA-EKF program is run again to check the accuracy of the speed estimation. Fig. 15 shows the phase voltage, phase current, and estimated speed of the motor. The mean-squared error of the estimated speed is found to be 1.7387, which is very close to the value obtained in the training phase.

VIII. CONCLUSION

This paper has presented a new method to optimize the performance of an EKF for speed estimation of an induction motor drive. Based on a real-coded GA, the optimization procedure enables the noise covariance and weight matrices, on which the EKF performance critically depends, to be properly selected. Simulation studies on two induction motor drives, namely, a constant V/Hz drive and an FOC drive, have confirmed the efficacy of the proposed approach. Experimental results obtained

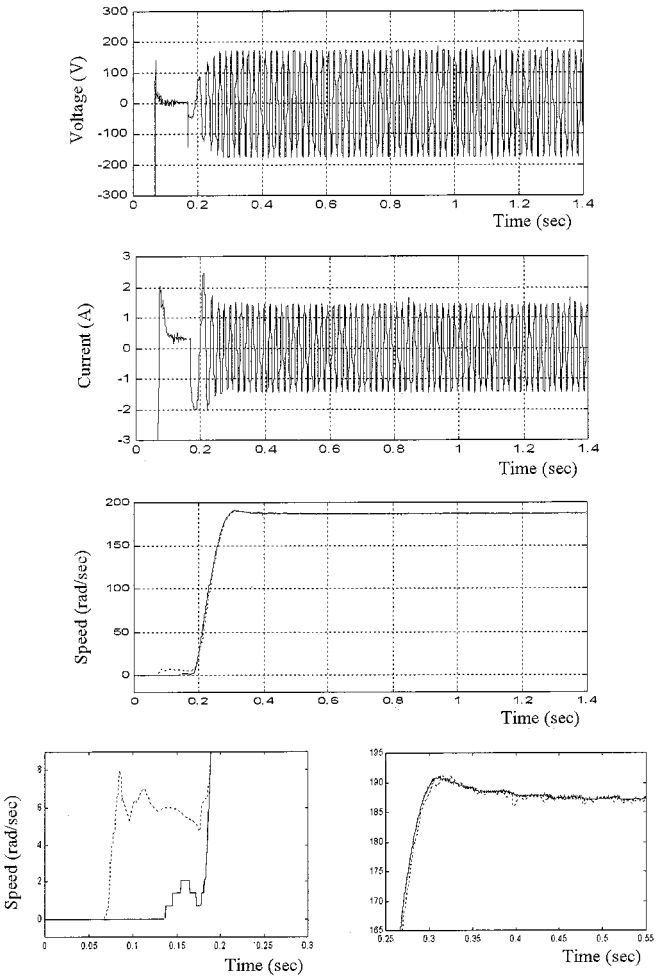

Fig. 15. Phase voltage, phase current, and speed estimated using the GA-optimized EKF when the motor is run up to 188 rad/s (solid line: actual speed; dotted line: estimated speed).

on a prototype FOC induction motor drive have verified the speed estimation accuracy of the optimized EKF. The work described has provided a basis for practical implementation of DSP-based sensorless induction motor drives in the future.

REFERENCES

[1] C. Manes, F. Parasiliti, and M. Tursini, "A comparative study of rotor flux estimation in induction motors with a nonlinear observer and the extended Kalman filter," in *Proc. IEEE IECON'94*, 1994, pp. 2149–2154.
[2] G. Henneberger, B. J. Brunsbach, and Th. Klepsch, "Field-oriented control of synchronous and asynchronous drives without mechanical sensors using a Kalman filter," in *Sensorless Control of AC Motor Drives*. New York: IEEE Press, 1996, pp. 207–214.
[3] Y. R. Kim, S. K. Sul, and M. H. Park, "Speed sensorless vector control of induction motor using extended Kalman filter," in *Sensorless Control of AC Motor Drives*. New York: IEEE Press, 1996, pp. 215–223.
[4] L. Salvatore, S. Stasi, and L. Tarchioni, "A new EKF-based algorithm for flux estimation in induction machines," *IEEE Trans. Ind. Electron.*, vol. 40, pp. 496–504, Oct. 1993.
[5] S. Bolognani, R. Oboe, and M. Zigliotto, "Sensorless full-digital PMSM drive with EKF estimation of speed and rotor position," *IEEE Trans. Ind. Electron.*, vol. 46, pp. 184–191, Feb. 1999.
[6] D. E. Goldberg, *Genetic Algorithms in Search, Optimization and Machine Learning*. New York: Addison-Wesley, 1989.
[7] A. H. Wright, "Genetic algorithms for real parameter optimization," in *Foundations of Genetic Algorithms*, J. E. Rawlins, Ed. San Mateo, CA: Morgan Kaufmann, 1991, pp. 205–218.
[8] F. L. Lewis, *Applied Optimal Control & Estimation*. New York: Prentice-Hall, 1992.

[9] K. L. Shi, T. F. Chan, Y. K. Wong, and S. L. Ho, "Speed estimation of induction motor using extended Kalman filter," in *Proc. IEEE Winter Meeting 2000*, vol. 1, Singapore, Jan. 23–27, 2000, pp. 243–248.
[10] C. M. Ong, *Dynamic Simulation of Electric Machinery Using Matlab/Simulink*. Upper Saddle River, NJ: Prentice-Hall PTR, 1998.
[11] D. B. Fogel, "Applying evolutionary programming to selected control problems," *Comput. Math. Applicat.*, vol. 11, no. 27, pp. 89–104, 1994.
[12] H. Muhlenbein and D. Schlierkamp-Voosen, "Predictive models for the Breeder Genetic Algorithm," *Evolutionary Computation*, vol. 1, no. 1, pp. 25–49, 1993.
[13] D. A. Linkens and H. O. Nyongesa, "Genetic Algorithms for fuzzy control," *Proc. IEE—Control Theory Applicat.*, vol. 142, no. 3, pp. 161–185, 1995.
[14] X. Xu and D. W. Novotny, "Implementation of direct stator flux orientation control on a versatile DSP based system," *IEEE Trans. Ind. Applicat.*, vol. 27, pp. 694–700, July/Aug. 1991.
[15] K. L. Shi, T. F. Chan, Y. K. Wong, and S. L. Ho, "Modeling and simulation of an induction motor," *Int. J. Elect. Eng. Educ.*, vol. 36, no. 2, pp. 163–172, 1999.

K. L. Shi received the B.Sc. degree from Chengdu University of Science and Technology, Chengdu, China, the M.Sc. degree from Harbin Institute of Technology, Harbin, China, and the Ph.D. degree in electrical engineering from the Hong Kong Polytechnic University, Hong Kong, in 1983, 1989, and 2001, respectively.

He is currently a Post-Doctoral Fellow in the Electrical and Computer Engineering Department, Ryerson Polytechnic University, Toronto, ON, Canada. His current research interests are intelligent control and estimation of induction motors.

T. F. Chan (M'95) received the B.Sc.(Eng.) and M.Phil. degrees in electrical engineering from the University of Hong Kong, Hong Kong, in 1974 and 1980, respectively.

Since 1978, he has been with the Department of Electrical Engineering, The Hong Kong Polytechnic University, Hong Kong, where he is currently an Associate Professor. His current research interests are self-excited ac generators, brushless ac generators, and computer-aided design of electrical machines.

Mr. Chan is a member of the Institution of Electrical Engineers, U.K., and the Hong Kong Institution of Engineers.

Y. K. Wong (M'80–SM'89) received the B.Sc. and M.Sc. degrees and the Dip.Ed. from London University, London, U.K., the M.Soc.Sc. degree from the University of Hong Kong, Hong Kong, the M.Phil. degree from the Chinese University of Hong Kong, Hong Kong, and the Ph.D. degree from Heriot-Watt University, Edinburgh, U.K.

In 1980, he joined The Hong Kong Polytechnic University, Hong Kong, where he is currently an Assistant Professor. His current research interests include linear systems, modeling, simulation, intelligent control, and power system control. He has authored more than 100 technical papers published in international journals and conference proceedings.

Dr. Wong is a Chartered Engineer, Chartered Mathematician, and Chartered Statistician in the U.K. He is a member of the Institution of Electrical Engineers, U.K., and a Fellow of the Institute of Mathematics and its Applications and the Royal Statistical Society.

S. L. Ho received the B.Sc. (First Class Honors) and Ph.D. degrees in electrical engineering from the University of Warwick, Warwick, U.K., in 1976 and 1979, respectively.

In 1979, he joined the Department of Electrical Engineering, The Hong Kong Polytechnic University, Hong Kong, where he is currently a Full Professor. He is very active in the areas of machine design, phantom loading of motors, condition monitoring of electrical machines, and traction engineering. He has authored more than 100 technical papers published in international journals and conference proceedings.